Available online at www.sciencedirect.com
SCIENCE DIRECT
Journal of Catalysis 238 (2006) 13–20
JOURNAL OF CATALYSIS
www.elsevier.com/locate/jcat

Structure, preparation and photocatalytic activity of titanium oxides on MCM-41 surface

Xuxu Wang [a], Wenhao Lian [a], Xianzhi Fu [a,*], Jean-Marie Basset [b], Frédéric Lefebvre [b,*]

[a] *Institute of Photocatalysis, University of Fuzhou, Gongye Lu 523, Fuzhou 350002, China*
[b] *Laboratoire de Chimie Organométallique de Surface, UMR CNRS-CPE 9986, 43 Bd du 11 Novembre 1918, 69616 Villeurbanne cédex, France*

Received 8 September 2005; revised 9 November 2005; accepted 21 November 2005

Available online 22 December 2005

Abstract

The grafting reaction of tetraneopentyl titanium on the surface of MCM-41 mesoporous molecular sieves dehydroxylated preliminary at 500 °C leads to formation of the well-defined bigrafted surface complex $(\equiv Si–O)_2Ti(CH_2CMe_3)_2$. On reaction with water or alcohol, the neopentyl ligands can be replaced selectively by alcoxy or hydroxy. On calcination at 500 °C, a well-dispersed titanium oxide supported on MCM-41 is obtained. In situ FTIR, DRS, and XAFS characterizations suggest that titanium is present as isolated tetrahedral species on the surface of MCM-41. This solid was used for the photocatalytic oxidation of ethylene in oxygen under UV irradiation, and its activity was compared to that of Ti-MCM-41 prepared by direct hydrothermal synthesis. The higher activity of the samples prepared by reaction with the organometallic complex is attributed to the good dispersion of titanium on the surface of MCM-41.

Keywords: MCM-41 molecular sieves; Tetraneopentyl titanium; Titanium oxide; Photocatalysis

1. Introduction

Titanium oxide is a well-known, extensively investigated semiconductor photocatalyst [1]. It has been established that the photocatalytic process in this compound results from the photoinduced electron–hole pairs, leading to highly active intermediate species such as O_2^-, $OH^\bullet$, $H^\bullet$, and the like [2]. Recently, molecular sieves containing some transition metal ions (most often titanium) within the framework were also found to be good photocatalysts [3–6].

The titanium oxide species prepared within the zeolite cavities and/or in the framework revealed a unique local structure, as well as high selectivity in the oxidation of organic substances with hydrogen peroxide [7,8]. But little is known about the chemical nature and the reactivity of these titanium oxide species, making it a challenge to synthesize well-defined catalytic sites that have photocatalytic activity. Synthesizing these sites would improve our knowledge of the photocatalytic process in these supported titanium catalysts.

One objective of surface organometallic chemistry is to immobilize organometallic complexes on solid surfaces such as oxides, zeolites, or metals to prepare well-defined surface species acting as highly selective heterogeneous catalysts [9]. For example, it is possible to stabilize on oxide surfaces some transition metal hydrides that are highly electron-deficient and have unusual catalytic activity, such as the low-temperature hydrogenolysis of acyclic alkanes, via activation of their C–H and C–C bonds [10].

In this work highly dispersed and well-defined titanium oxides on the surface of MCM-41 molecular sieves were prepared through surface organometallic chemistry and used for the photocatalytic oxidation of ethylene. The characterization of these catalysts by in situ IR, XRD, diffuse reflectance absorption, nitrogen adsorption, and XAFS (XANES and FT-EXAFS) measurements was done to clarify the characteristics of the photocatalytic oxidation of C_2H_4. Special attention has been focused on the relationship between the local structure and reactivity of the titanium oxide species.

* Corresponding authors. Fax: +86 591 8373 8608.
E-mail addresses: xzfu@fzu.edu.cn (X. Fu), lefebvre@cpe.fr (F. Lefebvre).

0021-9517/$ – see front matter
doi:10.1016/j.jcat.2005.11.027

2. Experimental

2.1. Synthesis of [Ti]-MCM-41

In a typical procedure derived from that described previously [11], three solutions containing titanium tetrabutoxide (TBOT), C_{16}TMABr, and sodium silicate were prepared. The solution of TBOT was first added to that of C_{16}TMABr under vigorous stirring at room temperature. Immediately afterward, the silicate solution was added, always under vigorous stirring. The pH was then adjusted to 8.5 by adding hydrochloric acid 1 M. The molar composition of the final mixture was x TBOT:1 SiO_2:0.67 Na_2O:0.2 C_{16}TMABr:102 H_2O:y HCl, with the x value corresponding to the desired amount of titanium in the resulting solid. After stirring for 3 h at room temperature, the gel mixture was autoclaved at 373 K for 24 h. The solid product was then filtered, washed several times with distilled water, and dried in air at 333 K. The template was removed by calcination at 813 K for 6 h in dry air. The resulting solid was denoted as [Ti]-19 (with the number corresponding to its Si/Ti atomic ratio). The pure siliceous MCM-41 used in the subsequent grafting reaction was synthesized without adding TBOT under the same conditions.

2.2. Preparation of MCM-41-TiNp$_x$ and Ti-MCM-41

The pure siliceous MCM-41 was first treated at 500 °C for 8 h under vacuum (10^{-4} Torr). When a deuterated sample was needed, the solid was allowed to contact with D_2O at 773 K for 2 h followed by a treatment under vacuum at the same temperature for 2 h. The procedure was repeated three times; the duration of the final vacuum treatment was 8 h. The resulting MCM-41 was more than 90% deuterated, as determined by quantitative IR data. $TiNp_4$ prepared as described previously [12], was sublimed in situ at 333 K on the dehydrated MCM-41. Elimination of unreacted complex was achieved by treatment under vacuum at this same temperature for 1 h. The efficiency of this procedure was checked by monitoring the experiment by IR spectroscopy until no significant variation of the intensity of the ν(C–H) bands could be detected. After hydrolysis, the solid was calcined under oxygen at 773 K for 6 h, producing a Ti-MCM-41 sample. Depending on the amount of complex introduced on the sample, three different materials—denoted as Ti-7, Ti-11, and Ti-22 (the number corresponding to their Si/Ti ratio)—were prepared.

2.3. Characterization

Gas-phase analysis of hydrocarbons was performed on a HP 5890 chromatograph equipped with a flame ionization detector and a HP-PLOT Al_2O_3 "S" column (50 m × 0.32 mm). Gases were expanded from IR cell into a small-lock chamber connected to the vacuum line and fitted with a rubber septum; N_2 was admitted to this chamber to atmospheric pressure just before GC analysis. Elemental analysis of samples was done by X-ray fluorescence spectroscopy (Philips PW2424F MagiX). Mass spectra were recorded on a quadrupole analyzer connected to a vacuum system capable of maintaining a residual pressure of 10^{-10} Torr.

The powder XRD patterns of all samples were measured on a Bruker Advance D8 X-ray powder diffractometer equipped with Cu-K_α radiation (40 kV, 40 mA). In general, the diffraction data were collected using a continuous scan mode with a scan speed of 0.6° 2θ/min over the range $1.5° < 2\theta < 10°$.

The UV–vis spectroscopic measurements in the 190–800 nm range were carried out on a Varian CARY 500 double-beam spectrometer equipped with an integrating sphere using $BaSO_4$ as a reference. All spectra were plotted in terms of $F(R)$ versus wavelengths. IR spectra were recorded on a Nicolet FT-IR 670 spectrometer equipped with a cell designed for in situ preparations under controlled atmosphere, using a self-supported MCM-41 disc.

Nitrogen adsorption–desorption measurements were carried out at 77 K on a Coulter Omnisorp 100 CX Sorptometer using a continuous-flow measurement mode. Before the measurements, the samples were outgassed at 333 K and 10^{-6} Torr for 6 h. Pore size distributions were calculated by the BJH method.

The X-ray absorption spectra (EXAFS and XANES) of the Ti-MCM-41 solids were acquired using Synchrotron Radiation provided by the NSRL (Hefei, China). The X-ray beam was emitted by a storage ring running at 0.8 GeV with a current of 80–250 mA. X-rays were monochromatized using a Si(111) two-crystal monochromator. The Ti K-edge spectra were recorded at room temperature in the transmission mode. The detection was carried out in two ion chambers, the first (I_0) was filled with N_2 and the second (I_1) filled with Ar/N_2. The spectra were processed conventionally. A linear background, determined by a least squares fitting of the pro-edge experimental points, was subtracted from the experimental spectrum. The maximum of the first peak of a titanium metal foil was then used as the energy reference. The resulting experimental data were analyzed with a chain of programs developed by the NSRL.

2.4. Catalytic experiments

The photocatalytic oxidation of ethylene was carried out in a tubular quartz reactor connected to a vacuum system. Catalyst samples of 50 mg were used for the test. Before photoreaction, the reactor was evacuated at room temperature for 1 h to remove air and CO_2 adsorbed on the catalyst, then filled with oxygen (101.325 kPa) and 500 µL C_2H_4 gas (with a C_2H_4 concentration of 320–330 ppm in oxygen). The tubular reactor was surrounded and illuminated by four 4 W fluorescent UV bulbs (Philips, main wavelength 254 nm) for 250 min. The reaction products in the gas phase were analyzed by gas chromatography with flame ionization and thermal conductivity detectors.

3. Results and discussion

3.1. Grafting reaction of tetraneopentyl titanium on MCM-41

When $TiNp_4$ was sublimed on a disk of MCM-41 dehydroxylated at 773 K, the resulting IR spectrum showed the

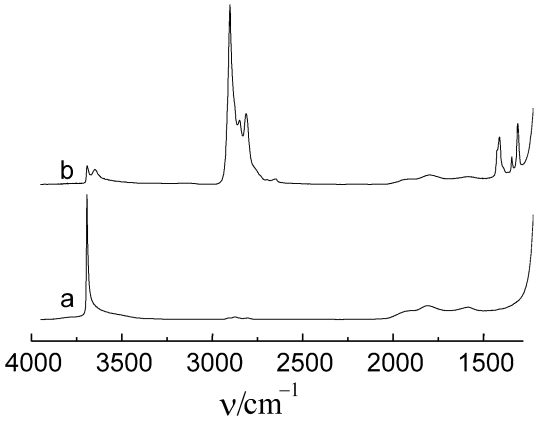

Fig. 1. Infrared spectra of MCM-41 activated at 773 K before (a) and after (b) reaction with tetraneopentyl titanium at 333 K and elimination of physisorbed species.

apparition of ν(C–H) and δ(C–H) vibrational bands, typical of neopentyl ligands, at 2954 ($\nu_{as}(CH_3)$), 2865 ($\nu_s(CH_2)$), 1464 ($\delta_{as}(CH_3)$), and 1363 cm^{-1} ($\delta_s(CH_3)$), with a strongly decreased intensity of the ν(O–H) band at 3740 cm^{-1} (Fig. 1). Simultaneously, neopentane evolved in the gas phase. But neopentane can arise from the reaction of the organometallic complex with surface hydroxyl groups or from the decomposition of tetraneopentyl titanium, which can occur during sublimation. To distinguish between these two effects, the reaction was also carried out on a MCM-41 sample preliminary deuterated (90% deuteration, as indicated by IR spectroscopy). The evolved neopentane was 90% monodeuterated, due to the reaction of the complex with the surface hydroxyl groups.

Chemical analysis showed that the amount of evolved neopentane per grafted titanium was 2.0 ± 0.2 whatever the amount of complex introduced on MCM-41. The same result was also obtained for larger samples (typically 0.5 g), demonstrating that there was no scale effect. We can then reasonably propose that the reaction of tetraneopentyl titanium with MCM-41 leads to the formation of a bigrafted titanium complex according to

$$TiNp_4 + 2(\equiv Si\text{–}OH) \rightarrow (\equiv Si\text{–}O)_2TiNp_2 + 2NpH\uparrow.$$

To confirm this structure, we studied the reactivity of $(\equiv Si\text{–}O)_2TiNp_2$ with several oxygenated molecules, typically methanol, water, and oxygen.

When $(\equiv Si\text{–}O)_2TiNp_2$ was reacted with methanol at room temperature (~20 kP), the silica disk, initially yellow, immediately turned white. The reaction was followed by in situ IR spectroscopy. The ν(C–H) and δ(C–H) vibrational bands characteristic of neopentyl ligands had disappeared completely and were replaced by new ν(C–H) (at 2957, 2926, 2872, 2853, and 2825 cm^{-1}) and δ(C–H) (at 1480, 1465, 1396, and 1366 cm^{-1}) bands that could be attributed to methoxy ligands. Simultaneously, neopentane was evolved in the gas phase, in nearly the same amount as in the grafting step (6.13×10^{-4} mol during the grafting step vs. 5.87×10^{-4} mol in methanolysis). Chemical analysis of the resulting solid gave Ti wt% = 2.8% and C wt% = 1.34%, corresponding to a molar C/Ti ratio of 1.9. These results are in agreement with the replacement of neopentyl ligands by methoxy ones, according to

$$(\equiv Si\text{–}O)_2TiNp_2 + 2CH_3OH \rightarrow (\equiv Si\text{–}O)_2Ti(OCH_3)_2 + 2NpH\uparrow.$$

Similarly, when the surface complex $(\equiv Si\text{–}O)_2TiNp_2$ was exposed to an excess of H_2O (22 kPa) at room temperature, the yellow solid quickly turned white. Simultaneously, the IR spectrum showed the appearance of bands typical of physical adsorbed water in the 4000–3000 cm^{-1} region and the disappearance of the ν(C–H) and δ(C–H) of neopentyl groups. As before, the amount of evolved neopentane was the same as that during the grafting reaction, corresponding to 2 neopentane per grafted titanium, whereas chemical analysis showed no carbon on the resulting solid. We can then reasonably propose that the following reaction occurred:

$$(\equiv Si\text{–}O)_2TiNp_2 + (n+2)H_2O \rightarrow (\equiv Si\text{–}O)_2Ti(OH)_2\cdot nH_2O + 2NpH\uparrow.$$

Finally, the surface complex $(\equiv Si\text{–}O)_2TiNp_2$ is very sensitive to trace amounts of O_2. Visible color change and IR spectroscopy indicated that the surface alkyl species reacted slowly with molecular oxygen at room temperature. The yellow solid became perfectly white over several hours. IR spectroscopy did not show drastic changes, in contrast to the foregoing studies, the ν(C–H) and δ(C–H) bands characteristic of neopentyl ligands shifted only slightly to higher wavenumbers. The gas phase contained no hydrocarbon, with chemical analysis demonstrating that all carbon had been retained on the surface. Davidson et al. showed that reaction of tetraneopentyl titanium with oxygen led to $Ti(ONp)_4$ [13]. In agreement with this finding and with preliminary studies on the reactivity of supported zirconium complexes with oxygen [14], we can then propose that the following reaction occurred with oxygen:

$$(\equiv Si\text{–}O)_2TiNp_2 + O_2 \rightarrow (\equiv Si\text{–}O)_2Ti(ONp)_2.$$

3.2. Synthesis of surface titanium oxides

The foregoing results show that $TiNp_4$ reacts with the surface hydroxyl of MCM-41 leading to well-defined $(\equiv Si\text{–}O)_2TiNp_2$ surface complexes. To synthesize the well-defined surface titanium oxide species, this surface complex was allowed to react first with water (to remove all organics) and was then heated under oxygen. The changes were monitored by IR spectroscopy as a function of temperature (Fig. 2). After treatment at moderate temperature, the IR spectrum in the 4000–3000 cm^{-1} region showed a wide band of hydrogen-bonded hydroxyl groups, which was wider than that of MCM-41 [15]. Its intensity decreased gradually under heating. Simultaneously, the band at 3740 cm^{-1} increased slightly. In this process, the hydrogen-bonded hydroxyl groups were transformed to isolated hydroxyl groups. It should also be pointed out that a band appeared at 3711 cm^{-1} and shifted to 3700 cm^{-1} when the heating temperature increased from 373 to 473 K. All of the hydrogen-bonded hydroxyl groups had disappeared at 623 K. In analogy with literature data [16,17], the

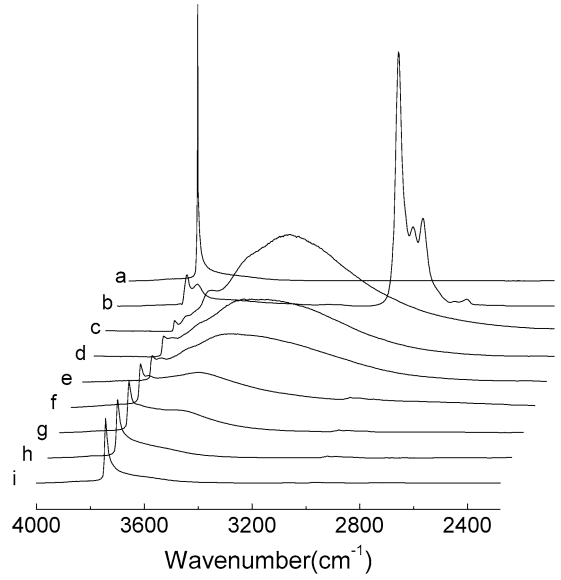

Fig. 2. Infrared changes with heating temperature of Ti-MCM-41 materials. MCM-41 dehydroxylated at 773 K (a); after reaction with $TiNp_4$ at 333 K (b); $+H_2O$ at 298 K (c); +evacuation under vacuum for 1 h at 298 K (d), 323 K (e), 373 K (f), 473 K (g), 623 K (h) and 773 K (i).

Table 1
Comparison of structural parameters of the various Titanium/MCM-41 samples after calcination at 773 K

Sample	Si/Ti ratio	*d*-value (nm)	Unit cell (nm)	BET surface area ($m^2\ g^{-1}$)	BJH average pore diameter (nm)
MCM-41	–	3.934	4.52	1001	3.0
[Ti]-19	19.0	3.806	4.37	895	2.78
Ti-22	22.8	3.897	4.48	949	2.97
Ti-11	11.1	3.893	4.47	931	2.94
Ti-7	7.1	3.874	4.45	919	2.88

bands at 3740, 3711, and 3700 cm^{-1} can be attributed to Ti–OH vibrations (the band at 3740 cm^{-1} is also due to isolated silanol groups).

3.3. Characterization of the different samples

Table 1 summarizes the structural properties of the Ti-substituted mesoporous molecular sieves prepared by the hydrothermal route (the one denoted as [Ti]-19) and by surface organometallic chemistry (those denoted as Ti-7, Ti-11, and Ti-22). The surface areas of all samples ranged from ca. 900 to ca. 1000 m^2/g, typical of M41S group materials (Fig. 3). For the three samples prepared from reaction with $TiNp_4$, the surface area decreased slightly with increasing amounts of titanium, probably related to the fact that the amount of mesoporous material per gram decreases as the amount of titanium increases. More interestingly, The BJH pore diameter of the three samples decreased slightly on the introduction of Ti, indicating that titanium atoms are located on the wall surfaces.

Fig. 4 shows XRD patterns of the various calcined Ti-mesoporous materials and the corresponding pure silicious MCM-41. Both the MCM-41 and Ti-mesoporous materials exhibited well-defined (100) reflections in their XRD patterns. These (100) reflections moved slightly to a high diffraction degree while long-range order diminished somewhat as Ti was incorporated. These results confirm that all materials retained the MCM-41 morphology and that, in the case of samples prepared by surface organometallic chemistry, the reaction with the organometallic complex had no effect on the silica support. For these samples, the combination of decreased pore size diameter and constant cell parameters indicates that an increase in the pore walls, corresponding to titanium at the surface or near the surface, while in the case of the hydrothermally sample titanium is located statistically in the walls.

The FTIR spectra of the titanium-grafted and hydrothermally prepared Ti-mesoporous molecular sieves clearly show a band at 960 cm^{-1}. For Ti-containing zeolites, this band at 960 cm^{-1} is believed to be a consequence of stretching vibrations of SiO_4 tetrahedral bound to the Ti atoms, that is, Si–O–Ti bonds and its systematic increasing intensity with increasing Ti content is generally taken as proof of the incorporation of titanium into the framework [18,19]. However, in our case this band is also present in the spectrum of pure MCM-41 and is related to the abundance of silanol groups present in the calcined samples [20]. Thus, the state of Ti on the surface of MCM-41 needs further characterization, such as UV–visible spectroscopy and XANES.

UV–vis DRS spectra of all samples are shown in Fig. 5. The spectra of the samples prepared by surface organometallic chemistry are clearly different from those of the samples prepared hydrothermally. This is demonstrated by the much broader absorption bands centered at 220 nm and 250–300 nm. The band at 220 nm is generally attributed to ligand-to-metal charge-transfer transition between the oxygen ligands to tetracoordinated Ti(IV) ions in the framework MCM-41 [19]. Its slight red shift for the samples prepared by reaction with $TiNp_4$ can be related to the fact that Ti species are in a distorted tetrahedral environment [21]. According to this assignment, the band at ca. 220 nm in Ti-MCM-41 may be associated with isolated Ti(IV) sites fundamentally similar in character to those in [Ti]-MCM-41. The shoulder at 270 nm probably corresponds to partially polymerized hexacoordinated Ti species and some Ti–O–Ti clusters are suspected to coexist with the isolated Ti sites in all of the samples [19]. The possibility cannot be ruled out that the Ti–O–Ti clusters are polymerized tetracoordinated Ti clusters (analogous TO_4 unit in MCM-41), corresponding to adsorption at wavelength of 220–270 nm. The spectra of Ti-7 and Ti-11 showed a red-shifted absorption band edge at 250–300 nm compared with that of Ti-22. The red shift was more prominent in Ti-7. This indicates that at least a fraction of the titanium in these materials is in octahedral coordination similar to that in TiO_2 particles [22]. In bulk titania, a broad absorption band occurs at 325 nm and is attributed to a O_2–Ti^{4+} charge transfer. No significant absorption at 300–350 nm was observed in our samples, suggesting that no segregated crystalline TiO_2 anatase phase is present in the Ti-MCM-41 [22]. In other words, our samples showed lower dispersion of Ti species than [Ti]-19, and their dispersion decreased with increasing amounts of Ti. This was confirmed by XANES spec-

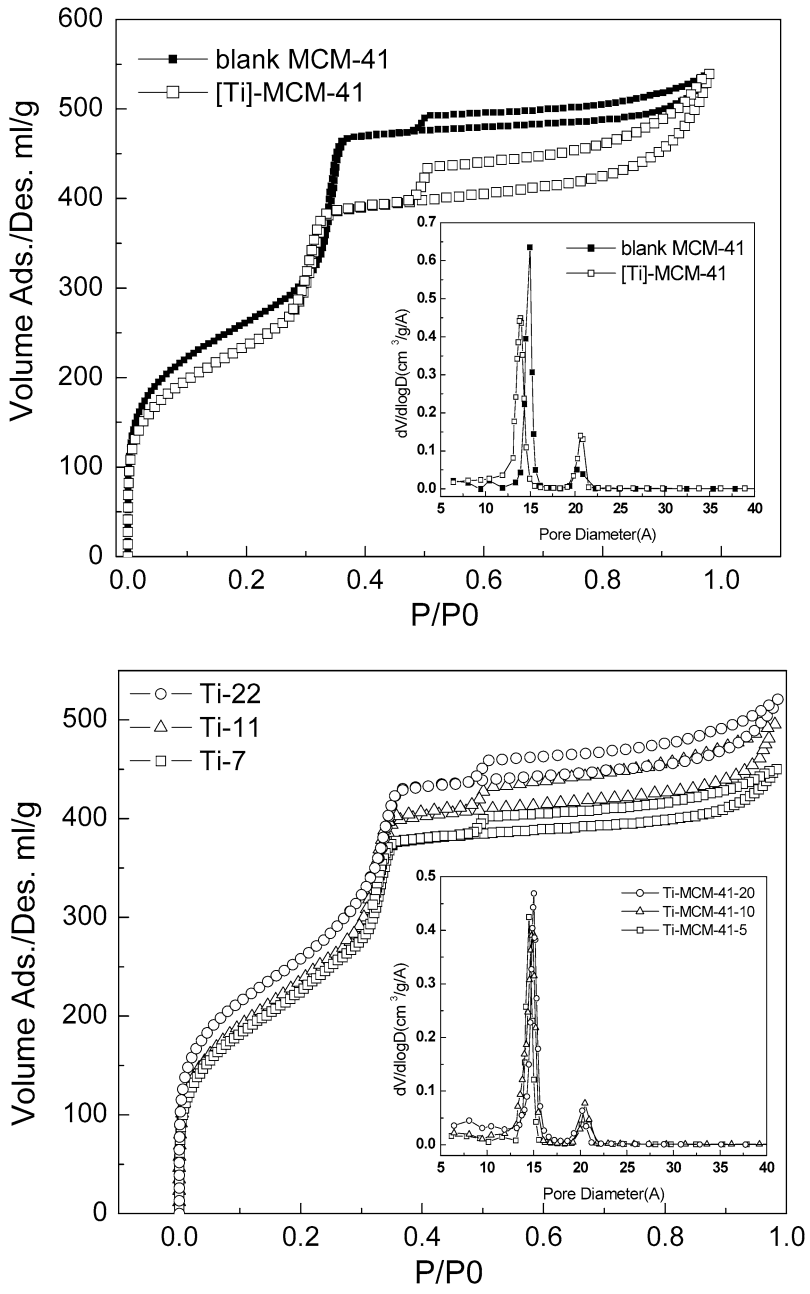

Fig. 3. Nitrogen adsorption–desorption isotherms and BJH pore radius of MCM-41, [Ti]-MCM-41 and Ti-MCM-41 samples.

tra showing rather weaker and broader pre-edge peaks of these samples compared with [Ti]-19 prepared by hydrothermal synthesis.

The XANES spectra of the [Ti]-MCM-41 and Ti-MCM-41 samples are shown in Fig. 6. To better elucidate the nature of the Ti sites in the solids, the Ti K-edge XANES spectra of reference compounds such as rutile are also given in this figure. In rutile, titanium is in octahedral coordination, and the XANES spectrum exhibits multiple, low-intensity pre-edge peaks at 4960–4980 eV. In contrast, tetrahedral Ti sites exhibit a single, high-intensity pre-edge peak [18]. Although tetrahedral and highly distorted octahedral Ti sites exhibit similar single pre-edge peaks, the two environments are clearly distinguishable by peak intensity and position.

The spectra of the [Ti]-MCM-41 and Ti-MCM-41 samples are very similar and contain a sharp pre-edge peak, and are quite different from the spectrum of rutile. The energy position of the pre-edge peak for Ti-MCM-41 samples is shifted slightly toward higher energies (and increased shift with increasing Ti content) compared with that of [Ti]-MCM-41, suggesting along with tetrahedral Ti the probable presence of some Ti in higher-coordination sites [21]. The intensity of the pre-edge peak for Ti-MCM-41 is also lower than that of [Ti]-MCM-41 and decreases with increasing Ti content. These experimental features clearly indicate a significant modification of the titanium coordination geometry from regular tetrahedron when the content of titanium increases. It can be reasonably posited that high titanium content will favor the formation of clusters with Ti–O–Ti

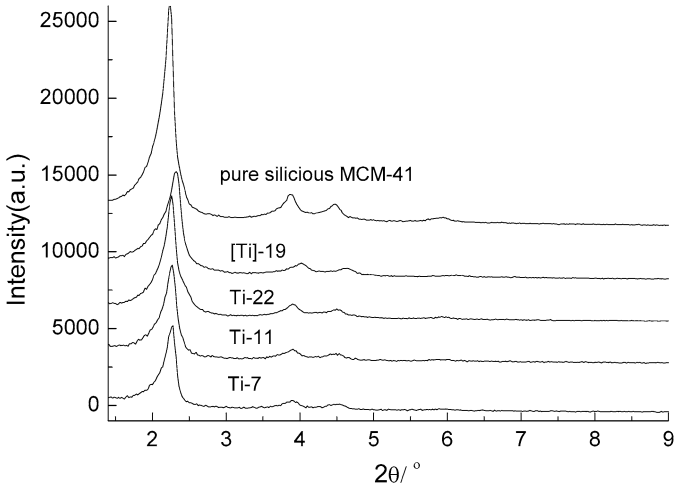

Fig. 4. XRD patterns of the various samples.

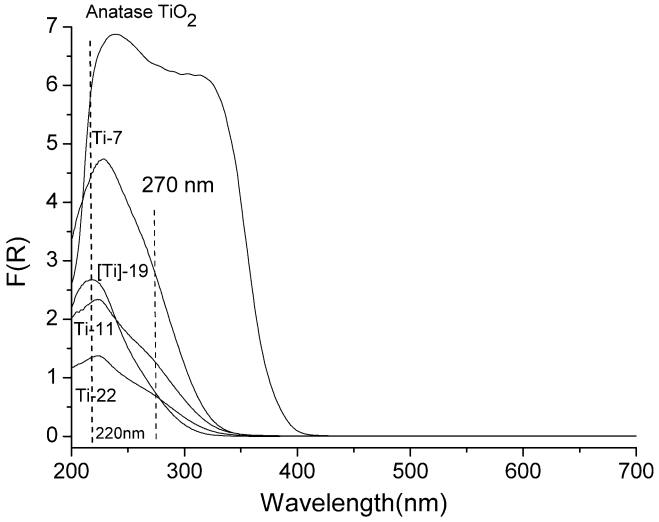

Fig. 5. Diffuse reflectance UV–vis spectra of the various samples.

bridges, even the clusters octahedrally coordinated with oxygen. In addition, the presence of water in a sample containing titanium induces an intensity decrease of the pre-edge absorption and a broadening of the peak. These observations are also supported by our UV–vis results.

To obtain further insight into the coordination environment of Ti, we analyzed the XAFS data of the calcined [Ti]-MCM-41 and Ti-MCM-41 samples; the results are shown in Figs. 7 and 8. The average Ti–O distance in a sixfold-coordinated silicate is between 1.94 Å [23] and ca. 2.06 Å [24]. In fresnoite ($Ba_2TiSi_2O_8$) with fivefold-coordinated Ti, the mean Ti–O distance is 1.92 Å [25]. The only crystalline model compound with tetrahedrally coordinated Ti is Ba_2TiO_4, with an average Ti–O distance of 1.81 Å [26]. For zeolites, the reported average Ti–O distances for fourfold-coordinated Ti in TS-1, TS-2, and Ti-Beta are in the range 1.80–1.88 Å [27]. The maximum of the first peak, corresponding to the first coordination shell around Ti, appears at 1.81 Å in Ti-22, 1.80 Å in [Ti]-19, and 1.94 Å in rutile. Clearly titanium is in tetrahedral coordination in Ti-22 and [Ti]-19. On increasing the Ti content (Fig. 8), the first peak

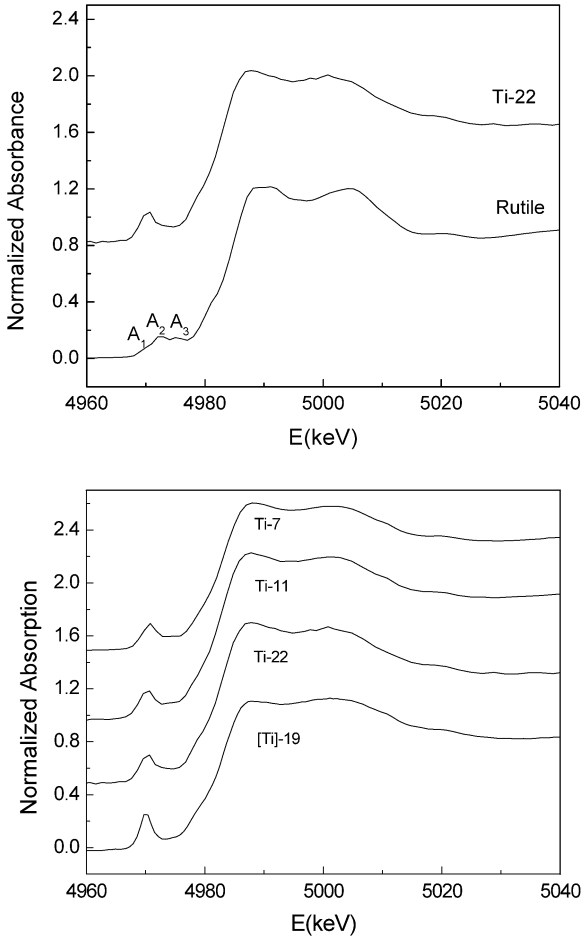

Fig. 6. Normalized Ti K-edge XANES spectra of rutile, [Ti]-19, Ti-22, Ti-11, and Ti-7.

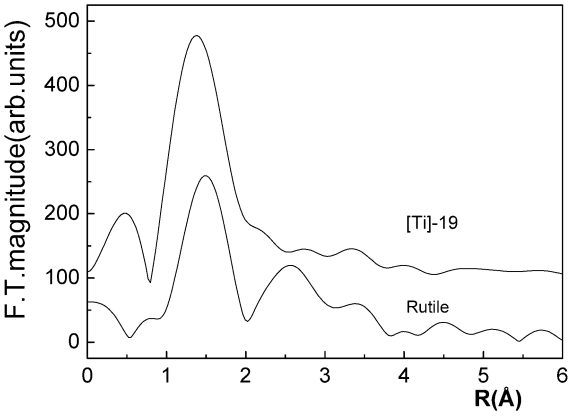

Fig. 7. EXAFS Fourier transforms of [Ti]-19 and rutile.

shifts to 1.89 Å for Ti-11 and 1.84 Å for Ti-7. This indicates that in these samples the amount of titanium in the higher coordination state increases, in agreement with the XANES and UV–vis results.

In summary, we can say that in the hydrothermally prepared sample, titanium is tetrahedrally coordinated and exists as isolated sites, whereas the situation is more complicated for the samples prepared by surface organometallic chemistry. If titanium is located on the wall surfaces in all cases, for low Ti

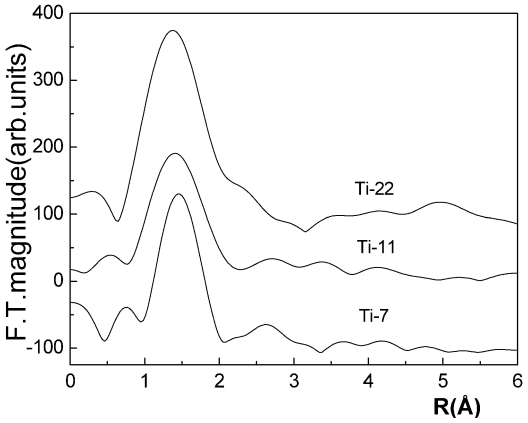

Fig. 8. EXAFS Fourier transforms of Ti-22, Ti-11 and Ti-7.

loadings (comparable to those achieved hydrothermally), Ti is in tetrahedral coordination, and for higher loadings, some titanium is present as clusters, probably in octahedral coordination.

3.4. Catalytic studies

The catalysts synthesized above were used in ethylene photocatalysis in presence of oxygen. For all samples, a formation of carbon dioxide and water was observed on UV irradiation, with yield increasing as a function of time. Under dark conditions, no products could be detected, showing that the formation of CO_2 and H_2O was due to a photocatalytic process. Fig. 9 shows the conversion and the yield of carbon dioxide for the four catalysts (pure MCM-41 is totally inactive for this reaction).

Comparing the activity of the Ti-22 and [Ti]-19 samples, which have nearly the same titanium content, clearly shows that the sample prepared by surface organometallic chemistry is more active. Because the state of titanium is near analogical for the two samples, the difference in activity is related to the amount of the active titanium species. All of the titanium is located on the wall surfaces for Ti-22, whereas titanium is partially on the surface for [Ti]-19. Consequently, the concentration of active tetrahedral titanium is higher using the preparation by reaction with $TiNp_4$. As the titanium concentration increases, ethylene conversion increases to its maximum level and then decreases slowly. As shown above, higher titanium loadings will lead to the formation of titanium oxide clusters, inactive for the reaction. Fig. 9 can then be considered a description of the amount of the active tetrahedral sites in the different solids. As discussed in Section 3.3, the large tail band at high titanium content is difficult to quantitatively identify, but there is evidence that the photocatalytic activity is related to the tetrahedral titanium species, including the isolated ones and polymerized tetracoordinated titanium cluster.

Titanium-containing mesoporous silica as a photocatalyst has also been studied by other groups. Anpo et al. prepared Ti-containing HMS with varying Ti contents by a hydrothermal method and compared their photocatalytic activity for the decomposition of NO. The photocatalytic activity of a sample depended on its Ti amount; that is the lower the Ti content,

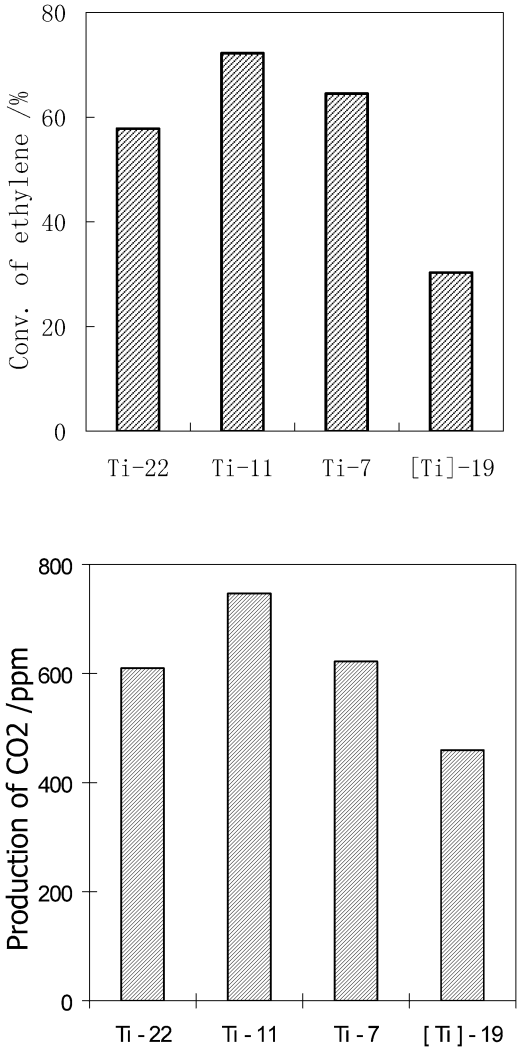

Fig. 9. Photocatalytic oxidation: conversion of ethylene and yield of CO_2 over [Ti]-19, Ti-22, Ti-11 and Ti-7.

the higher the photocatalytic activity. This was ascribed to the differences in the Ti coordination environment. Ti atoms occupied site-isolated positions in the frameworks at low loadings and were in a distorted tetrahedral environment or octahedral coordination sphere at higher loadings. The authors suggested that the charge-transfer excited state of the tetrahedrally coordinated titanium oxide species plays a significant role in the direct photocatalytic decomposition of NO into N_2 [28]. They generalized this supposition to the photocatalytic process occurring on the transition metal oxides incorporated within the framework of zeolites [29]. Note that our samples have obvious differences from Anpo et al.'s Ti-HMS samples. [Ti]-19 has only ca. 0.05 wt% of Ti, whereas Ti-HMS (1) (the Ti-HMS with the lowest Ti loading) contained ca. 1 wt% of Ti. Moreover, the content of Ti in our Ti-x samples is <0.2 wt%, and Ti exists only on the surface. It is reasonable to suggest that the major portion of titanium ions exists as $Ti(SiO_4)_4$ units in framework for [Ti]-19, because it has lower Ti content than Ti-HMS (1). In contrast with [Ti]-19, Ti ions in Ti-x samples must not exist as $Ti(SiO_4)_4$ units on the surface. Both our results and the findings of Anpo et al. show that Ti ions existing in tetrahedral coordi-

nation are photocatalytically active with oxygen, but our results emphasize that only the tetrahedrally coordinated titanium with oxygen on the surface is responsible for the photocatalytic behavior based on the difference in activity between [Ti]-19 and Ti-22. But the characterizations given here remain incomplete for the identification of the state of all Ti ions, and the some questions remain unanswered, including how many Ti ions are on the surface for samples prepared by the thermal route and how many of them exist as isolated TiO_4 units for samples prepared by surface organometallic chemistry, The possibility of Ti–O–Ti tetrahedral coordination clusters anchored on the surface cannot be excluded. The answers to these questions depend on quantitative identification of the surface Ti species. Some characterizations by UV–Raman spectroscopy and XPS for the samples are currently in progress and will be published elsewhere.

4. Conclusion

The tetrahedrally coordinated Ti highly dispersed on the surface of MCM-41 can be prepared using surface organometallic chemistry. These Ti-MCM-41 catalysts exhibit high photocatalytic activity in the oxidation of C_2H_4. Our results indicate that the highly dispersed Ti, in tetrahedral coordination, plays a significant role in photocatalytic oxidation. The chemical state of Ti depends on the grafting Ti content. At high Ti content, octahedral-coordinated titanium as Ti–O–Ti oxides are present, decreasing the photocatalytic activity.

Although the detailed reaction mechanism behind the present reaction merits further investigation, our results strongly indicate that mesoporous zeolites with highly dispersed titanium oxide species prepared on the surface by organometallic chemistry are promising photocatalysts.

Acknowledgments

This work was supported by the National Natural Science Foundation of China (grants 20173009, 20373011, 20133010, 20573020, 20537010), the National Key Basic Research Special Foundation of China (grant 2004CCA07100), and the Natural Science Foundation of Fujian, China (grant 2003F004). The authors thank Faqiang Xu and Shiqiang Wei, National Synchrotron Radiation Laboratory (University of Science and Technology of China, Hefei), for collection and discussion of the EXAFS data.

References

[1] M.R. Hoffmann, S.T. Martin, W. Choi, D.W. Bahnemann, Chem. Rev. 95 (1995) 69.
[2] M. Anpo, Y. Kubokawa, Rev. Chem. Intermed. 8 (1987) 105.
[3] M. Anpo, S.G. Zhang, H. Yamashita, Stud. Surf. Sci. Catal. 39 (1996) 431.
[4] S.G. Zhang, Y. Ichihashi, H. Yamashita, T. Tatsumi, M. Anpo, Chem. Lett. (1996) 895.
[5] Y. Ichihashi, H. Yamashita, M. Anpo, Stud. Surf. Sci. Catal. 105 (1997) 1609.
[6] B. Notari, Adv. Catal. 41 (1996) 253.
[7] T. Tatsumi, M. Nakamura, S. Negishi, H. Tominaga, J. Chem. Soc., Chem. Commun. (1990) 476.
[8] J.S. Reddy, R. Kumar, J. Catal. 130 (1991) 440.
[9] F. Lefebvre, J.M. Basset, Curr. Top. Catal. 3 (2002) 215.
[10] J. Corker, F. Lefebvre, C. Lecuyer, V. Dufaud, F. Quignard, A. Choplin, J. Evans, J.M. Basset, Science 271 (1996) 966.
[11] X.X. Wang, F. Lefebvre, J. Patarin, J.M. Basset, Microporous Mesoporous Mater. 42 (2001) 269.
[12] W. Mowat, G. Wilkinson, J. Chem. Soc., Dalton Trans. (1973) 1120.
[13] P.J. Davidson, M.F. Lappert, R.J. Pearce, J. Organomet. Chem. 57 (1973) 269.
[14] M. Adachi, C. Nedez, X.X. Wang, F. Bayard, V. Dufaud, F. Lefebvre, J.M. Basset, J. Mol. Catal. A: Chem. 204–205 (2003) 443.
[15] J.S. Chen, Q.H. Li, R.R. Xu, F.S. Xiao, Angew. Chem. Int. Ed. Engl. 34 (1995) 23.
[16] K.E. Lewis, G.D. Parfitt, Trans. Faraday Soc. 62 (1966) 204.
[17] P. Jackson, G.D. Parfitt, Trans. Faraday Soc. 67 (1971) 2469.
[18] T. Blasco, A. Corma, M.T. Navarro, J.P. Pariente, J. Catal. 156 (1995) 65.
[19] W.S. Ahn, D.H. Lee, T.J. Kim, J.H. Kim, G. Seo, R. Ryoo, Appl. Catal. 181 (1999) 39.
[20] M.R. Boccuti, K.M. Rao, A. Zecchina, G. Leofanti, G. Petrini, in: G. Morterra, A. Zecchina, G. Casle (Eds.), Structure and Reactivity in Surfaces, Elsevier, Amsterdam, 1989, p. 133.
[21] W.Z. Zhang, F. Michael, J.L. Wang, T.T. Peter, J. Wong, J.P. Thomas, J. Am. Chem. Soc. 118 (1996) 9164.
[22] A.M. Prakash, M.S. Hyung, K. Larry, J. Phys. Chem. B 102 (1998) 857.
[23] K. Fischer, Z. Kristallogr. 129 (1969) 222.
[24] E. Canillo, F. Mazzi, G. Rossi, Acta Crystallogr. 21 (1966) 200.
[25] P.B. Moore, S.J. Louisnathan, Z. Kristallogr. 130 (1969) 439.
[26] K.K. Wu, I.D. Brown, Acta Crystallogr. Sect. B 29 (1973) 2009.
[27] T. Dumas, J. Petiau, J. Non-Cryst. Solids 81 (1986) 201.
[28] J. Zhang, M. Minagaw, T. Ayusaw, S. Natarajan, H. Yamashit, M. Matsuok, M. Anpo, J. Phys. Chem. B 104 (2000) 11501.
[29] M. Matsuok, M. Anpo, J. Photochem. Photobiol. C: Photochem. Rev. 3 (2003) 225.